JACS
JOURNAL OF THE AMERICAN CHEMICAL SOCIETY
Article
pubs.acs.org/JACS

Reticular Synthesis of HKUST-like tbo-MOFs with Enhanced CH_4 Storage

Ioannis Spanopoulos,[†] Constantinos Tsangarakis,[†] Emmanuel Klontzas,[†] Emmanuel Tylianakis,[§] George Froudakis,[†] Karim Adil,[‡] Youssef Belmabkhout,[‡] Mohamed Eddaoudi,[‡] and Pantelis N. Trikalitis*[,†]

[†]Department of Chemistry and [§]Department of Materials Science and Technology, University of Crete, Voutes Campus, 71003 Heraklion, Greece

[‡]Functional Materials Design, Discovery & Development (FMD[3]), Advanced Membranes & Porous Materials Center, Division of Physical Sciences and Engineering, King Abdullah University of Science and Technology (KAUST), P.O. Box 4700, Thuwal 23955-6900, Kingdom of Saudi Arabia

Supporting Information

ABSTRACT: Successful implementation of reticular chemistry using a judiciously designed rigid octatopic carboxylate organic linker allowed the construction of expanded HKUST-1-like **tbo**-MOF series with intrinsic strong CH_4 adsorption sites. The Cu-analogue displayed a concomitant enhancement of the gravimetric and volumetric surface area with the highest reported CH_4 uptake among the **tbo** family, comparable to the best performing metal organic frameworks (MOFs) for CH_4 storage. The corresponding gravimetric (BET) and volumetric surface areas of 3971 m^2 g^{-1} and 2363 m^2 cm^{-3} represent an increase of 115% and 47%, respectively, in comparison to the corresponding values for the prototypical HKUST-1 (**tbo**-MOF-1), and are 42% and 20% higher than that of **tbo**-MOF-2. High-pressure methane adsorption isotherms revealed a high total gravimetric and volumetric CH_4 uptakes, reaching 372 cm^3 (STP) g^{-1} and 221 cm^3 (STP) cm^{-3}, respectively, at 85 bar and 298 K. The corresponding working capacities between 5 and 80 bar were found to be 294 cm^3 (STP) g^{-1} and 175 cm^3 (STP) cm^{-3} and are placed among the best performing MOFs for CH_4 storage particularly at relatively low temperature. To gain insight on the mechanism accounting for the resultant enhanced CH_4 storage capacity, molecular simulation study was performed and revealed the presence of very strong CH_4 adsorption sites near the organic linker with similar adsorption energetics as the open metal sites. The present findings support the potential of **tbo**-MOFs based on the supermolecular building layer (SBL) approach as an ideal platform to further enhance the CH_4 storage capacity via expansion and functionalization of the quadrangular pillars.

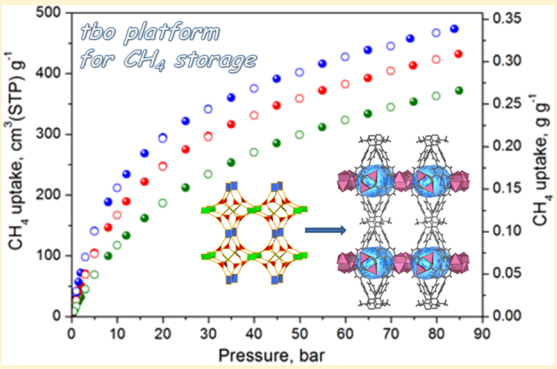

INTRODUCTION

The utilization of fossil fuels in the energy production and the mobile transportation sector results in the emission of massive amounts of CO_2 in the atmosphere, instigating numerous health and environmental issues.[1] Thus, prompt deployment of environmental friendly fuels is of utmost importance. Natural gas, consisting of nearly 95% CH_4, is a good candidate for replacing gasoline in mobile transportation and coal in stationary power plants, since it can sustain the same energy demand with amply lessened release of CO, CO_2, NO_x, and SO_2 pollutants.[2] Nevertheless, the deployment of methane as a typical fuel in the automotive industry has been hindered by practicalities associated with cost-effective and efficient storage of methane at concrete temperatures and pressures.[3]

Metal organic frameworks (MOFs) represent an exceptional class of functional solid-state materials suitable for numerous applications, due to their unique modularity, unprecedented tunability, and high degree of porosity combined with diverse framework functionalities.[4] Accordingly, MOF chemistry offers great potential to address challenging issues pertaining to CH_4 storage.[3b,5] As an illustration of a MOF compound with high promise for CH_4 storage, HKUST-1[6] was reported to be the best performing material at intermediate pressures (35−65 bar), showing a total volumetric uptake of 267 cm^3 (STP) cm^{-3} at 298 K and 65 bar with a corresponding working capacity (5−65 bar) of 190 cm^3 (STP) cm^{-3}.[7] Although HKUST-1 exhibits remarkable performance in comparison to the best storage media, it is still far below the gravimetric and volumetric DOE target of 0.5 g/g and 264 cm^{-3}/cm^{-3} in the range of temperatures between −40 and 85 °C, typical for a vehicle in real operation.[3b,8]

Received: October 22, 2015

DOI: 10.1021/jacs.5b11079
J. Am. Chem. Soc. XXXX, XXX, XXX−XXX

Successful implementation of reticular chemistry and the molecular building block approach offers nowadays a potential to ideally target MOFs with desired and appropriate structural features. For example, HKUST-1[9] material that has an underlying **tbo**-a topology can be further interpreted and regarded as constructed from a 2-periodic arrays of squares, each consistent with an augmented 4,4 square lattice (**sql**-a), that are cross-linked through 4-connected pillars containing copper paddlewheels. This underlying layer, isolated through deconstruction of the crystal structure, can be targeted and constructed from judiciously selected metals and ligands. Then, rational design using pillaring strategy, also called supermolecular building layer (SBL) approach,[10] can be readily implemented using appropriately selected organic pillars that permit the generation of the anticipated 3-periodic MOF. Based on this background and rationally, it is conceivable to reasonably target/synthesize an expanded or/and functionalized HKUST-l like **tbo**-MOF with higher gravimetric and volumetric surface area which in turn will result in a relatively higher CH_4 uptake.

The SBL approach has first been introduced and employed by Eddaoudi et al. to construct a new family of isoreticular MOFs with **tbo** topology by using quadrangular (octatopic) organic ligands instead of trigonal (tritopic) ones as in the case of HKUST-1.[10] The use of quadrangular organic ligands offers the advantages to modulate porosity and functionalization of the resulting material, but most importantly, it prevents self-interpenetration as it is observed in the case of MOF-388.[11] In this way it is possible to efficiently utilize extended organic ligands and synthesize tailor-made **tbo**-MOF materials with specific pore size and volume. So far, there are only a few examples of **tbo**-MOFs fabricated from quadrangular organic ligands[12] and studied for CH_4 storage.

The first attempt to fabricate a high surface area HKUST-like **tbo**-MOF was achieved using tetra-isophthalate ligand connected through methoxy groups to a 4-connected benzene core[10,13] (see Scheme S2). Although the surface area and pore volume were improved, the strategy of extending the pillars without introduction of functional groups led unfortunately to a decrease in the total and working CH_4 gravimetric and volumetric uptake in the 35−65 bar range, as this strategy induces the removal of dimeric paddlewheel units carrying strong CH_4 adsorption sites (see Scheme S3).[13] Therefore, maintaining adequate high CH_4 interaction sites associated with the surface area and pore volume increase is not straightforward, particularly in the case of the **tbo**-MOF platform. Accordingly, it was compelling for us to explore the use of SBL strategy to develop novel HKUST-1 like **tbo**-MOFs with extended linkers having strong CH_4 interaction sites.

To address this challenge, it is important to note that a **tbo**-based structure requires an isophthalate-based octatopic organic linker (four isophthalate groups) with specific geometrical constrains that limit the choice of suitable organic linkers.[12b] To overcome these limitations, two different strategies could provide a suitable pathway to construct the targeted MOF: (i) the use of flexible octatopic linkers that has been proven to be a successful strategy[10] but in turn jeopardizes the framework stability due to the increased strain energy of the ligand[12b] and (ii) the employment of highly aromatic, rigid octatopic organic pillars that can maintain/enhance the stability of the material and also increase CH_4 uptake through favorable $\pi\cdots CH_4$ interactions. Moreover, these interactions could be further enhanced by functionalizing the aromatic rings with methyl groups. It is evident that this strategy is highly challenging and implies the design and synthesis of new, highly aromatic rigid octatopic linkers suitable for the formation of expanded **tbo**-MOFs.

Indeed, we designed and synthesized the rigid octatopic organic linker 3,6-dimetheyl-1,2,4,5-tetra-(biphenyl-3′,5′-dicarboxylic acid)benzene (H_8L) shown in Figure 1, which upon

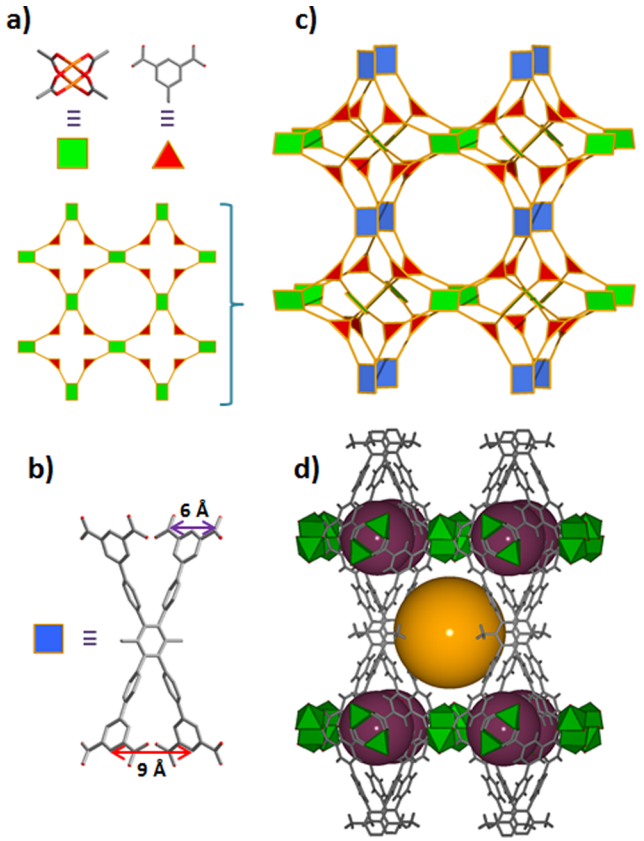

Figure 1. (a) Assembly of 4-connected square-like paddlewheel and 3-connected triangle-like BTC to generate 2-periodic 4,4-connected augmented square lattice (**sql**-a). (b) Octatopic linker (H_8L) acting as 4-connected node. (c) The **tbo**-a topology. (d) Crystal structure of Cu-**tbo**-MOF-5 showing two types of cavities.

solvothermal reaction in the presence of Co^{2+}, Cu^{2+}, and Zn^{2+} readily afforded the desired **tbo**-MOFs. We reasoned that the presence of two methyl groups attached to the central phenyl ring is beneficial because it will increase the electron density of this ring, which will induce the CH_4-framework interaction enhancement at this site and in turn, will augment the total CH_4 storage capacity, and will reduce the relatively large size of the central structure cavity, keeping in this way the overall porosity at the micropore region.

Here we show that while the Co-**tbo**-MOF-5 and Zn-**tbo**-MOF-5 MOFs were found unstable upon solvent removal, due to the resultant incompatible coordination geometry of the metal center, the Cu-**tbo**-MOF-5 showed excellent structural stability and methane sorption capabilities. Notably, in comparison with HKUST-1, the present expanded Cu-**tbo**-MOF-5 analogue displays a 115% and 47% increase in the gravimetric and volumetric surface area, respectively.[14] Detailed CH_4 adsorption measurements revealed that Cu-**tbo**-MOF-5 exhibits very high gravimetric and volumetric storage capacities reaching 372 cm^3 (STP) g^{-1} (0.266 g g^{-1}) and 221 cm^3 (STP)

DOI: 10.1021/jacs.5b11079
J. Am. Chem. Soc. XXXX, XXX, XXX−XXX

cm^{-3} respectively, at 85 bar and 298 K. The gravimetric working capacity between 5 and 80 bar at 298 K is 294 cm^3 (STP) g^{-1} (0.217 g g^{-1}). This value surpasses two of the currently best performing MOFs for CH_4 storage, HKUST-1[7] (0.162 g g^{-1}) and MOF-519[6] (0.172 g g^{-1}) and places Cu-**tbo**-MOF-5 among the best performing MOFs for CH_4 storage. Quantum chemistry calculations and Monte Carlo simulations confirmed the experimental results and shed light on CH_4-framework interactions that helped to better understand the observed CH_4 adsorption mechanism.

RESULTS AND DISCUSSION

The design of new, large, and rigid quadrangular isophthalate-based organic linkers for the construction of expanded **tbo**-MOFs necessitates to define the appropriate geometrical attribute to readily pillar the 2-periodic layers. The in-deep analysis of the structure reveals that the distance between the neighboring isophthalate groups of the organic moieties, indicated in Figure 1b by the red arrow, is of prime importance for the fabrication of the targeted MOF. Indeed, as the distance between the carboxylates belonging to an isophthalic moiety is almost fixed, ~ 6 Å, the required distance between two neighboring isophthalates has to be ~9 Å to accommodate the distance between two paddlewheels from the 2-periodic layers. The use of such an organic linker with the adequate distance and consequently with the appropriate conformation will allow the generation of the desired **tbo**-MOF with no conformational change of the ligand and will in fine result in relatively more stable structure.[12b] The successful synthesis of the designed ligand, as shown in Figure 2, allowed us to fabricate the desired **tbo**-MOFs. Indeed, solvothermal reaction between $\mathbf{H_8L}$ and $Co(NO_3)_2{\cdot}6H_2O$, $Cu(NO_3)_2{\cdot}3H_2O$ or $Zn(NO_3)_2{\cdot}6H_2O$ readily afforded the construction of the corresponding MOFs with the expected **tbo** topology. These MOFs are denoted here as Co-**tbo**-MOF-5, Cu-**tbo**-MOF-5, and Zn-**tbo**-MOF-5, respectively. Powder X-ray diffraction analysis (PXRD) indicated that the three MOFs are isostructural compounds (see Figure S7).

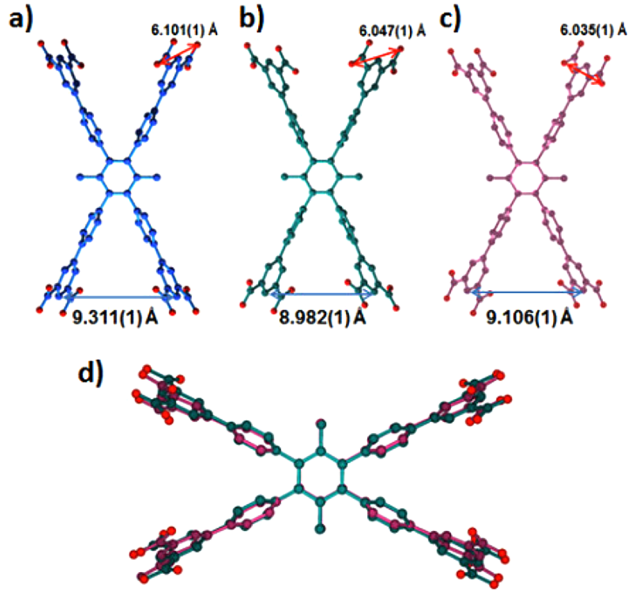

Figure 2. The structure of $\mathbf{H_8L}$ linker (a) as predicted by DFT, (b) in Cu-**tbo**-MOF-5, and (c) in Zn-**tbo**-MOF-5. (d) Overlay of the DFT-predicted structure of the ligand and that found in Cu-**tbo**-MOF-5, showing that there is only a small change in the dihedral angle of the isophthalate groups, when $\mathbf{L}^{8-}$ is incorporated into the **tbo** framework.

Initially, single crystals were isolated only in the case of Zn-**tbo**-MOF-5 (colorless plates, see Figure S5), while Co-**tbo**-MOF-5 and Cu-**tbo**-MOF-5 were isolated in a microcrystalline form. Remarkably, green plate-like single crystals of Cu-**tbo**-MOF-5 were obtained in a high quality through a facile, single-crystal-to-single-crystal topotactic and quantitative exchange of Zn^{2+} by Cu^{2+} (see Supporting Information (SI)). The quantitative replacement of Zn^{2+} by Cu^{2+} was confirmed by EDS (see Figure S6). The structure of Zn-**tbo**-MOF-5 and Cu-**tbo**-MOF-5 was determined by single crystal X-ray diffraction experiments (see Table S1 and S2). The purity of these materials has been confirmed by comparison between the experimental and calculated PXRD patterns (see Figure S7). Given that both **tbo** MOFs are isostructural, the structure of Cu-**tbo**-MOF-5 will be presented in more detail below.

Cu-**tbo**-MOF-5 crystallizes in the orthorhombic system, space group *Fmmm* with large unit cell parameters, a = 25.616(2) Å, b = 28.157(3) Å, and c = 40.549(4) Å resulting in a unit cell volume of 29247(5) $Å^3$. The corresponding volume of Zn-**tbo**-MOF-5 was found slightly bigger, reaching 29811(10) $Å^3$, as expected due to the slightly longer Zn−O bond length. As expected from the **tbo**-type structure, the framework consists of dimeric paddlewheel $[M_2(O_2C-)_4$, M = Cu^{2+} and $Zn^{2+}]$ units in which the metal cations exhibit a square pyramidal MO_5 geometry (see Figure 1). These 4-connected paddlewheels are linked to each other's through isophthalic moieties of the ligand, resulting in a neutral 3-periodic framework with microporous cavities of different sizes (see Figure 1). Precisely, the larger cavity, ~16 Å in length, along the c-axis is located between the layers (see orange sphere in Figure 1) which has two different widths along the a-axis due to the different arrangement of the central phenyl ring carrying the two methyl groups, pointing alternatively inside and outside of the cavity. A smaller cavity, ~11 Å in length, exists within the layers (see green sphere in Figure 1).[15] The size of these cavities was further confirmed experimentally by accurate microporous analysis in the case of Cu-**tbo**-MOF-5 using Ar at 87 K. The total solvent accessible free volume for Cu-**tbo**-MOF-5 was found to be 73%, using the PLATON software.[16]

Proper activation of the Cu-**tbo**-MOF-5 was successfully achieved by applying a straightforward activation procedure using volatile solvents such as acetone and CH_2Cl_2 to exchange the DMF molecules followed by drying under vacuum and heating at 60 °C overnight (see SI). In contrast, all attempts to properly activate Co-**tbo**-MOF-5 and Zn-**tbo**-MOF-5 using available methodologies such as supercritical CO_2 drying failed and lead to a systematic structural collapse. The origin of such phenomena can be directly correlated to the unstable distorted square planar MO_4 geometry (M = Co^{2+}, Zn^{2+}) resulting from the paddlewheels desolvation under the activation process. Accordingly, upon activation, the coordinated solvent molecules located at the apical positions of the paddlewheels are removed resulting in four coordinated metal centers. The formation of stable paddlewheel units SBUs necessitates that metal centers adopt a square planar geometry. Although for Cu^{2+} the 4-connected square planar environment is a stable geometry with carboxylate-based ligands, it is not the case for Co^{2+} and Zn^{2+} cations which both prefer/adopt the more stable tetrahedral geometry.[12f] The latter destroys the dimeric paddlewheels leading to the collapse of the framework.[12c]

DOI: 10.1021/jacs.5b11079
J. Am. Chem. Soc. XXXX, XXX, XXX−XXX

Argon adsorption isotherm recorded at 87 K confirmed the permanent porosity of Cu-**tbo**-MOF-5 showing a fully reversible type-I isotherm, characteristic of a microporous material, see Figure 3. The BET (Langmuir) surface area,

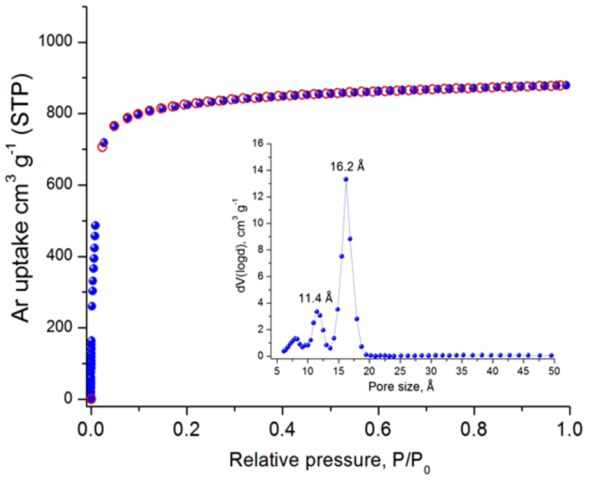

Figure 3. Argon sorption isotherm at 87 K for Cu-**tbo**-MOF-5 and the corresponding pore size distribution curve calculated by NLDFT.

calculated in the pressure range 0.007−0.01 p/p$_0$, was found to be 3971 m^2 g^{-1} (4123 m^2 g^{-1}), which is more than double (115%) compared to the prototypical **tbo** MOF, HKUST-1 (BET area, 1850 m^2 g^{-1})[7] and 37% higher than **tbo**-MOF-2.[10,13] Taking into account the crystallographic density of Cu-**tbo**-MOF-5 (ρ = 0.595 g cm^{-3}), the calculated volumetric BET area is 2363 m^2 cm^{-3}, which is significantly higher (47%) compared to the corresponding value of HKUST-1 (ρ = 0.868 g cm^{-3}, 1606 m^2 cm^{-3}). The calculated geometric surface area using the nonorthoSA software[17] (probe diameter 3.4 Å) is 3850 m^2 g^{-1}, which is very close to the experimental BET value and confirms that Cu-**tbo**-MOF-5 framework retains its structural integrity upon pore system activation. This is also supported by the total pore volume calculated from the Ar adsorption isotherm at 0.992 p/p$_o$ that it is found to be 1.12 cm^3 g^{-1}, which is in close agreement with the crystallographic value of 1.22 cm^3 g^{-1}. In addition to gas-sorption results, the structural integrity of activated Cu-**tbo**-MOF-5 was also confirmed by PXRD measurements (see Figure S8). The pore size distribution was calculated using non-local density functional theory (NLDFT) after a successful fitting of the Ar adsorption isotherm data using a suitable NLDFT kernel (see Figure S11). Accordingly, the corresponding curve (see inset in Figure 3) shows two distinct peaks centered at 16.2 and 11.4 Å, in full agreement with the crystallographic analysis. Thermogravimetric analysis (TGA) and variable-temperature powder X-ray diffraction (VT-PXRD) measurements demonstrate that Cu-**tbo**-MOF-5 is stable up to 250 °C (see Figures S26 and S27).

The high gravimetric and volumetric surface area, due to the large pore volume in the micropore region, in combination with the high degree of aromaticity, the methyl groups at the central ring, and the presence of unsaturated Cu^{2+} sites make Cu-**tbo**-MOF-5 a very promising material for gas storage. Accordingly, extensive CH$_4$ sorption measurements at different temperatures and pressures were performed in order to evaluate the Cu-**tbo**-MOF-5 in terms of key CH$_4$ properties including the saturation uptake, total uptake, working capacity, and isosteric heat of adsorption. CH$_4$ adsorption measurements recorded at its boiling point (112 K) and up to 1 bar showed a fully reversible type-I isotherm, with a high saturation uptake of 691 cm^3 (STP) g^{-1}, (404 cm^3 (STP) cm^{-3}), see Figure S12. The total pore volume calculated at 0.99 p/p$_0$ using CH$_4$ as a probe molecule is 1.17 cm^3 g^{-1} and is in excellent agreement with both the experimental value obtained from Ar adsorption (1.2 cm^3 g^{-1}) at 87 K and the calculated from the crystal structure (1.22 cm^3 g^{-1}), indicating that the pore space in Cu-**tbo**-MOF-5 is fully accessible by CH$_4$ molecules. From the CH$_4$ adsorption isotherms recorded at 273, 283, and 298 K, the calculated isosteric heat of adsorption at zero coverage, Q_{st}^0, using a virial-type equation was estimated to be 20.4 kJ mol^{-1} and remained nearly constant as a function of the surface coverage (see Figure S15). Interestingly, this value is higher compared to HKUST-1 (17 kJ mol^{-1}) and among the highest reported for MOFs (see Table S1).[5a] For example, Ni-MOF-74 with very high density of open metal sites showed a Q_{st}^0 value of 21.4 kJ mol^{-1}. As we described in detail below, accurate theoretical calculations revealed that in Cu-**tbo**-MOF-5, in addition to the open Cu^{2+} sites, there are three distinct sites with interaction strength equal to that of open Cu^{2+} sites (~20 kJ mol^{-1}), reasoning the observed high Q_{st}^0 value.

High-pressure CH$_4$ measurements at different temperatures, shown in Figure 4, revealed that Cu-**tbo**-MOF-5 exhibited one

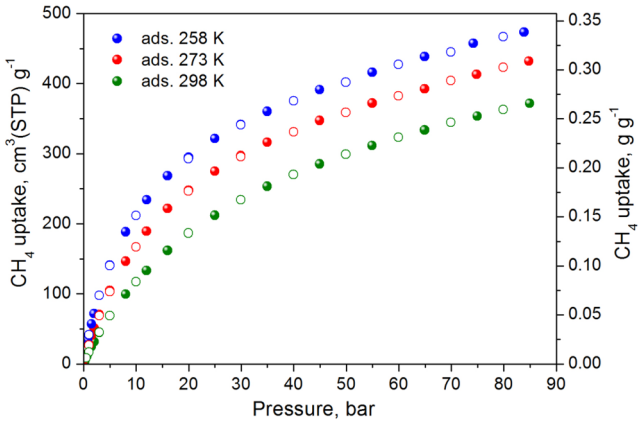

Figure 4. Total gravimetric CH$_4$ adsorption (closed symbols) and desorption (open symbols) isotherms of Cu-**tbo** at the indicated temperatures.

of the highest gravimetric uptakes for MOFs, reaching 372 cm^3 (STP) g^{-1} (0.266 g g^{-1}) at 85 bar and 298 K. The corresponding values at 273 and 258 K are 432 cm^3(STP) g^{-1} (0.309 g g^{-1}) and 473 cm^3 (STP) g^{-1} (0.338 g g^{-1}), respectively. The latter is 67.7% of the current gravimetric DOE target, 700 cm^3 (STP) g^{-1} (0.5 g g^{-1}). The gravimetric working capacity between 5 and 80 bar at 298 K is 294 cm^3 (STP) g^{-1} (0.217 g g^{-1}) which surpasses two of the best performing MOFs for CH$_4$ storage, HKUST-1 and MOF-519, showing 227 cm^3 (STP) g^{-1} (0.162 g g^{-1}) and 241 cm^3 (STP) g^{-1} (0.172 g g^{-1}),[6] respectively, under the same conditions (see Figure 5a and Tables S1 and S2). It is also higher compared to other high expanded **tbo**-MOFs like **tbo**-MOF-2, as shown in Figure S24 (253 cm^3 g^{-1} vs 225 cm^3 g^{-1} at 35 bar and 298 K).[13] Using the crystal density of Cu-**tbo**-MOF-5 (0.595 g cm^{-3}), the calculated total volumetric uptake at 85 bar and 298, 273, and 258 K is 221, 257, and 282 cm^3 (STP) cm^{-3}, respectively. The corresponding volumetric working capacities between 5 and

DOI: 10.1021/jacs.5b11079
J. Am. Chem. Soc. XXXX, XXX, XXX−XXX

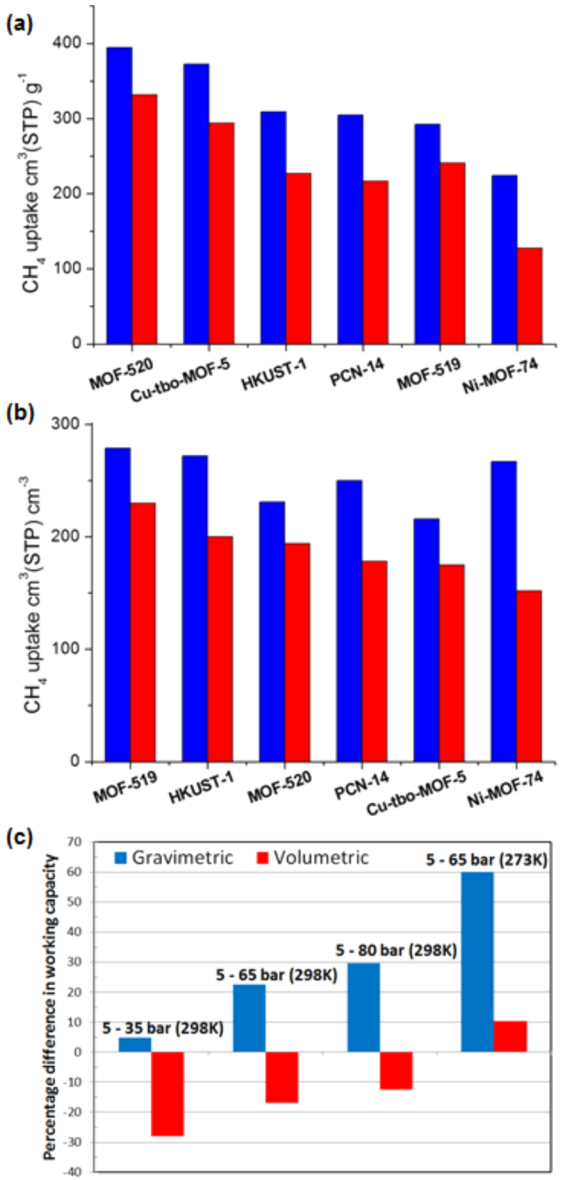

Figure 5. Comparison of (a) gravimetric and (b) volumetric CH_4 total uptake (blue) at 80 bar/298 K and the corresponding working capacities (red) between 5 and 80 bar/298 K, of Cu-**tbo**-MOF-5 with some top performing MOFs. (c) Percentage difference in gravimetric (blue) and volumetric (red) working capacities between Cu-**tbo**-MOF-5 and HKUST-1 at the indicated pressure ranges and temperatures.

80 bar are 175, 189, and 194 cm^3 (STP) cm^{-3}. These values compare well with the best performing MOFs as shown in Figure 5b (see also Table S2).[7,18] Interestingly, although Cu-**tbo**-MOF-5 has a significantly higher volumetric surface area compared to the prototypical **tbo** MOF, HKUST-1, the latter showed a higher volumetric working capacity, 200 cm^3 (STP) cm^{-3} between 5 and 80 bar at 298 K that is mainly attributed to the considerably higher (~46%) crystal density of HKUST-1 (0.868 g cm^{-3}).

A detailed comparison of CH_4 storage properties in terms of working capacities between HKUST-1 and Cu-**tbo**-MOF-5 revealed important findings. In fact, Cu-**tbo**-MOF-5 shows higher gravimetric working capacity between 5 and 65 bar (more relevant to real applications than the 5−35 bar range due to the upper limit achievable with inexpensive two-stage compressors) by 22.7% at 298 K, while in the range 5−80 bar, the corresponding increase is 29.6%. The volumetric working capacity shows a decrease of 16.8% in the range of 5−65 bar but a much lower decrease, 12.5%, in the range of 5−80 bar, both at 298 K. Because a temperature decrease has a similar effect in CH_4 uptake as the increase in pressure, it is relevant to compare the corresponding CH_4 working capacities between the two solids at a lower temperature. Remarkably, at 273 K the volumetric working capacity in the range of 5−65 bar is increased by 10.3% (the percentage difference between 298 and 273 K is 27.1%), while the gravimetric working capacity shows an impressive increase of 60.1%. These results are shown in Figure 5c.

A very rare behavior is noticed in Cu-**tbo**-MOF-5. Indeed, the increase of both gravimetric and volumetric working capacity is observed as the temperature is decreasing, which is the opposite for HKUST-1 and other high performance MOFs including UTSA-76 and NU-111. This kind of dependence of the working capacity suggests that a combination of pressure and temperature swing could be an effective method for methane storage and release.[19] For example, using Cu-**tbo**-MOF-5, an adsorption at 258 K at 65 bar, followed by a desorption at 5 bar and 298 K, will result in a volumetric working capacity of 220 cm^3(STP) cm^{-3} which is 83% of the DOE target (264 cm^3 cm^{-3}), if the packing loss is ignored.

The above results could originate from the synergistic effect between pore volume (this correlates with surface area) and CH_4-framework interactions. Accordingly, due to higher pore volume and moderate CH_4-framework interactions in Cu-**tbo**-MOF-5, the uptake is smaller in the low-pressure region (5 bar range) compared to the high-pressure range (see Figure 4), leading in this way to higher working capacities. The opposite is true for HKUST-1, where pore confinement due to smaller pore volume results in increased CH_4 uptake at lower pressures and saturation close to 65 bar (see Figure S24).

Computational methods were employed with the aim to identify the CH_4 adsorption sites in Cu-**tbo**-MOF-5 and in particular, to better understand the effect of the various structural features of the extended **tbo**-type framework on the observed CH_4 storage properties. Accordingly, quantum chemistry calculations and Monte Carlo simulations with the grand canonical ensemble (GCMC) were performed in order to investigate the energetics of the CH_4 adsorption and to simulate adsorption isotherms at different conditions. Interestingly, the calculations showed that Cu-**tbo**-MOF-5 possesses four highly energetic CH_4 adsorption sites of equal strength (~20 kJ mol^{-1}), indicated as **I**, **II**, **III**, and **IV** in Figure 6 and one more, **V**, with relatively lower interaction energy (15 kJ mol^{-1}). More specifically, in addition to the open Cu^{2+} sites (**II**), usually being energetically the highest interaction sites in MOFs, there are three more, **I**, **III**, and **IV**, of equal strength, located at the positions shown in Figure 6. As expected from the **tbo** topology, **I**, **II**, and **III** are the most energetic ones, similarly to HKUST-1.[20] However, it is interesting to highlight that sites **IV** and **V** are also found to be highly energetic because of the particular structure of the ligand. The high adsorption strength of the **IV** site is attributed to the local geometry of the small v-shaped pocket of the ligand and the subsequent increased dispersion interactions of the CH_4 molecule ($\pi\cdots$H−C interactions) with the opposite aromatic rings (see Figure 6). Less energetic, but important in terms of its strength (~15 kJ mol^{-1}), is site **V** at the top of the central phenyl ring of the ligand carrying the two methyl groups. The

DOI: 10.1021/jacs.5b11079
J. Am. Chem. Soc. XXXX, XXX, XXX−XXX

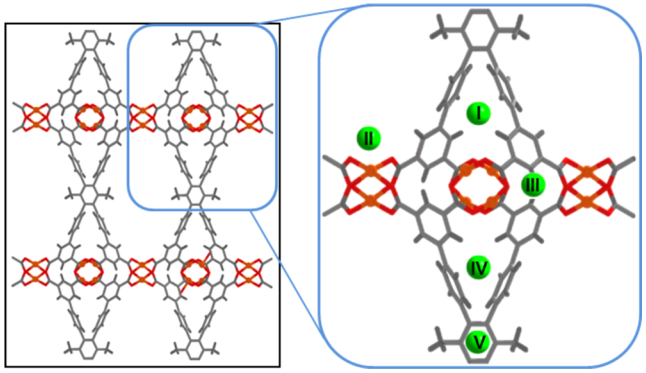

Figure 6. Five major CH_4 adsorption sites in Cu-**tbo**-MOF-5. The sites **I**–**IV** have the same interaction strength of ~20 kJ mol^{-1}, while the site **V** has 15 kJ mol^{-1}. Site **I** is located at the window entrance of the octahedral cage, site **II** at the axial position of the Cu^{2+} paddlewheel, site **III** between the carboxylate groups inside the cage, site **IV** at the v-shaped pocket formed by the neiboring arms of the ligand, and site **V** at the top of the central phenyl ring of the ligand carrying the two methyl groups.

calculations showed that the origin of the amplified strength of this site, as compared to the other phenyl rings of the ligand (~10 kJ mol^{-1}), is the electron-donating nature of the two methyl groups. In addition, due the orientation of the organic ligand, these groups are pointing inside the large cavity of the structure, creating in this way a window of ~8 Å which favors $CH_4\cdots CH_4$ and CH_4-framework interactions.[21] This is supported by the calculations which showed that with the loading augmentation, an additional increase of ~2 kJ mol^{-1} to the average adsorption strength is observed, apparently due to favorable $CH_4\cdots CH_4$ interactions. These results are in full agreement with the experimental Q_{st} values and also explain the slight increase of Q_{st} as a function of surface coverage at low pressures (between 0 and 1 bar) (see Figure S15). GCMC simulations slightly overestimate (8%) the total gravimetric CH_4 uptake at high pressures (see Figure S32) which notably correlates very well with the difference between the observed (1.12 cm^3 g^{-1}) and calculated total pore volume (1.22 cm^3 g^{-1}) of Cu-**tbo**-MOF-5.

In addition to CH_4, H_2 and CO_2 sorption measurements were performed in the low-pressure region (0–1 bar) at various temperatures. Accordingly, H_2 adsorption at 77 K revealed an impressive uptake of 261 cm^3 (STP) g^{-1} (2.3 wt %) at 1 bar with a Q_{st}^0 of 6.3 kJ mol^{-1} (see Figures S21 and S19). A very high CO_2 uptake was also found, reaching at 273 and 298 K and 1 bar, 149 cm^3 (STP) g^{-1} (6.6 mmol g^{-1}) and 80 cm^3 (STP) g^{-1} (3.6 mmol g^{-1}), respectively (see Figure S17). The corresponding Q_{st} at zero coverage, determined for the isotherms recorded at 273, 283, and 298 K, is estimated to be 24.5 kJ mol^{-1} and found to be constant as a function of the surface coverage, indicating the presence of uniform CO_2-framework interactions in Cu-**tbo**-MOF-5 (see Figure S18). Using the IAST model, the calculated CO_2/CH_4 selectivity at 273 and 298 K for a 5/95 molar mixture is 5.1 and 4.2, respectively (see Figure S20).

CONCLUSIONS

In conclusion, we have demonstrated how reticular chemistry and more specifically the SBL approach can allow the synthesis of a new series of **tbo**-MOFs with significantly enhanced gravimetric and volumetric surface area, compared to the prototype **tbo** MOF, HKUST-1. The design of an original expanded, highly aromatic, and rigid organic linker with intrinsically strong CH_4 adsorption sites allowed the isolation of a new very stable porous MOF, namely Cu-**tbo**-MOF-5, that shows very high gravimetric and volumetric BET surface area, reaching 3971 m^2 (STP) g^{-1} and 2363 m^2 cm^{-3}, respectively. Extensive gas adsorption measurements, at various temperatures and pressures, revealed that Cu-**tbo**-MOF-5 is currently among the best performing MOFs for CH_4 storage, showing a gravimetric total uptake of 372 cm^3 (STP) g^{-1} at 85 bar and 298 K, which is higher than that of HKUST-1 and MOF-519, and also an impressive volumetric total capacity of 221 cm^3 (STP) cm^{-3}, under the same conditions (working capacity between 5 and 80 bar, 175 cm^3 cm^{-3}). Theoretical calculations of the CH_4 adsorption in Cu-**tbo**-MOF-5 revealed the presence of multiple strong adsorption sites of equal strength with the open Cu^{2+} sites (~20 kJ mol^{-1}), which concurs with the experimentally determined isosteric heat of adsorption. The increased strength of these sites originates from both the particular structural features of the ligand and the **tbo**-MOF structural features, **tbo** topology. These significant results provide new directions for the design and construction of novel **tbo**-MOFs with further improved CH_4 storage properties, namely with enhanced volumetric total and working capacities, while maintaining a high density of strong interaction sites.

ASSOCIATED CONTENT

Supporting Information

The Supporting Information is available free of charge on the ACS Publications website at DOI: 10.1021/jacs.5b11079.

Experimental details, powder XRD, NMR, TGA, gas-sorption isotherms and related calculations (PDF)
Crystallographic data (CIF)
Crystallographic data (CIF)

AUTHOR INFORMATION

Corresponding Author

*ptrikal@uoc.gr

Notes

The authors declare no competing financial interest.

ACKNOWLEDGMENTS

The authors thank Diamond Light Source for access to beamline I19 (MT10189) that contributed to the results presented here and in particular for the determination of Cu-**tbo**-MOF-5 structure and also D. Allan and H. Nowell for their assistance during the measurements. We also thank HZB for the allocation of synchrotron radiation beamtime, used to solve the Zn-**tbo**-MOF-5 structure. This research has been cofinanced by the European Union (European Social Fund, ESF) and Greek national funds through the Operational Program "Education and Lifelong Learning" of the National Strategic Reference Framework (NSRF) Research Funding Program: ARISTEIA II - 4862. Part of this work was supported by King Abdullah University of Science and Technology (KAUST).

REFERENCES

(1) (a) Markewitz, P.; Kuckshinrichs, W.; Leitner, W.; Linssen, J.; Zapp, P.; Bongartz, R.; Schreiber, A.; Muller, T. E. *Energy Environ. Sci.* **2012**, *5* (6), 7281–7305. (b) Liu, C.; Li, F.; Ma, L. P.; Cheng, H. M. *Adv. Mater.* **2010**, *22* (8), E28. (c) D'Alessandro, D. M.; Smit, B.;

DOI: 10.1021/jacs.5b11079
J. Am. Chem. Soc. XXXX, XXX, XXX–XXX

Long, J. R. *Angew. Chem., Int. Ed.* **2010**, *49* (35), 6058−6082. (d) Li, S.-L.; Xu, Q. *Energy Environ. Sci.* **2013**, *6* (6), 1656−1683.
(2) Lozano-Castello, D.; Alcaniz-Monge, J.; de la Casa-Lillo, M. A.; Cazorla-Amoros, D.; Linares-Solano, A. *Fuel* **2002**, *81* (14), 1777−1803.
(3) (a) Beckner, M.; Dailly, A. *Appl. Energy* **2015**, *149*, 69−74. (b) Mason, J. A.; Veenstra, M.; Long, J. R. *Chem. Sci.* **2014**, *5* (1), 32−51.
(4) (a) Yaghi, O. M.; O'Keeffe, M.; Ockwig, N. W.; Chae, H. K.; Eddaoudi, M.; Kim, J. *Nature* **2003**, *423* (6941), 705−714. (b) Furukawa, H.; Cordova, K. E.; O'Keeffe, M.; Yaghi, O. M. *Science* **2013**, *341*, 6149. (c) Almeida Paz, F. A.; Klinowski, J.; Vilela, S. M. F.; Tome, J. P. C.; Cavaleiro, J. A. S.; Rocha, J. *Chem. Soc. Rev.* **2012**, *41* (3), 1088−1110. (d) Assen, A. H.; Belmabkhout, Y.; Adil, K.; Bhatt, P. M.; Xue, D.-X.; Jiang, H.; Eddaoudi, M. *Angew. Chem., Int. Ed.* **2015**, *54*, 14353−14358. (e) Xue, D.-X.; Belmabkhout, Y.; Shekhah, O.; Jiang, H.; Adil, K.; Cairns, A. J.; Eddaoudi, M. *J. Am. Chem. Soc.* **2015**, *137*, 5034. (f) Lu, W.; Wei, Z.; Gu, Z.-Y.; Liu, T.-F.; Park, J.; Park, J.; Tian, J.; Zhang, M.; Zhang, Q.; Gentle, T., III; Bosch, M.; Zhou, H.-C. *Chem. Soc. Rev.* **2014**, *43* (16), 5561−5593. (g) Guillerm, V.; Kim, D.; Eubank, J. F.; Luebke, R.; Liu, X.; Adil, K.; Lah, M. S.; Eddaoudi, M. *Chem. Soc. Rev.* **2014**, *43*, 6141.
(5) (a) He, Y.; Zhou, W.; Qian, G.; Chen, B. *Chem. Soc. Rev.* **2014**, *43* (16), 5657−5678. (b) Elizabeth Casco, M.; Martinez-Escandell, M.; Gadea-Ramos, E.; Kaneko, K.; Silvestre-Albero, J.; Rodriguez-Reinoso, F. *Chem. Mater.* **2015**, *27* (3), 959−964. (c) Alezi, D.; Belmabkhout, Y.; Suetin, M.; Bhatt, P. M.; Weselinski, L. J.; Solovyeva, V.; Adil, K.; Spanopoulos, I.; Trikalitis, P. N.; Emwas, A.-H.; Eddaoudi, M. *J. Am. Chem. Soc.* **2015**, *137* (41), 13308−13318.
(6) Gandara, F.; Furukawa, H.; Lee, S.; Yaghi, O. M. *J. Am. Chem. Soc.* **2014**, *136* (14), 5271−5274.
(7) Peng, Y.; Krungleviciute, V.; Eryazici, I.; Hupp, J. T.; Farha, O. K.; Yildirim, T. *J. Am. Chem. Soc.* **2013**, *135* (32), 11887−11894.
(8) *Methane Opportunities for Vehicular Energy (MOVE)*, Funding Opportunity no. DE-FOA-0000672, Advanced Research Project Agency-Energy (ARPA-E), U.S. Department of Energy: Washington, DC, 2012.
(9) O'Keeffe, M.; Peskov, M. A.; Ramsden, S. J.; Yaghi, O. M. *Acc. Chem. Res.* **2008**, *41* (12), 1782−1789.
(10) Eubank, J. F.; Mouttaki, H.; Cairns, A. J.; Belmabkhout, Y.; Wojtas, L.; Luebke, R.; Alkordi, M.; Eddaoudi, M. *J. Am. Chem. Soc.* **2011**, *133* (36), 14204−14207.
(11) Furukawa, H.; Go, Y. B.; Ko, N.; Park, Y. K.; Uribe-Romo, F. J.; Kim, J.; O'Keeffe, M.; Yaghi, O. M. *Inorg. Chem.* **2011**, *50* (18), 9147−9152.
(12) (a) Lu, W.; Yuan, D.; Makal, T. A.; Li, J.-R.; Zhou, H.-C. *Angew. Chem., Int. Ed.* **2012**, *51* (7), 1580−1584. (b) Shustova, N. B.; Cozzolino, A. F.; Dinca, M. *J. Am. Chem. Soc.* **2012**, *134* (48), 19596−19599. (c) Wei, Z.; Lu, W.; Jiang, H.-L.; Zhou, H.-C. *Inorg. Chem.* **2013**, *52* (3), 1164−1166. (d) Yang, X.-L.; Xie, M.-H.; Zou, C.; He, Y.; Chen, B.; O'Keeffe, M.; Wu, C.-D. *J. Am. Chem. Soc.* **2012**, *134* (25), 10638−10645. (e) Yang, X.-L.; Zou, C.; He, Y.; Zhao, M.; Chen, B.; Xiang, S.; O'Keeffe, M.; Wu, C.-D. *Chem. - Eur. J.* **2014**, *20* (5), 1447−1452.
(13) Belmabkhout, Y.; Mouttaki, H.; Eubank, J. F.; Guillerm, V.; Eddaoudi, M. *RSC Adv.* **2014**, *4* (109), 63855−63859.
(14) Chui, S. S. Y.; Lo, S. M. F.; Charmant, J. P. H.; Orpen, A. G.; Williams, I. D. *Science* **1999**, *283* (5405), 1148−1150.
(15) A detailed and representative description of the different cavities formed in **tbo**-type MOFs is provided in ref 10.
(16) Spek, A. L. *Acta Crystallogr., Sect. D: Biol. Crystallogr.* **2009**, *65*, 148−155.
(17) Dueren, T.; Millange, F.; Ferey, G.; Walton, K. S.; Snurr, R. Q. *J. Phys. Chem. C* **2007**, *111* (42), 15350−15356.
(18) Gutov, O. V.; Bury, W.; Gomez-Gualdron, D. A.; Krungleviciute, V.; Fairen-Jimenez, D.; Mondloch, J. E.; Sarjeant, A. A.; Al-Juaid, S. S.; Snurr, R. Q.; Hupp, J. T.; Yildirim, T.; Farha, O. K. *Chem. - Eur. J.* **2014**, *20* (39), 12389−12393.
(19) (a) Sun, B.; Kayal, S.; Chakraborty, A. *Energy* **2014**, *76*, 419−427. (b) Kayal, S.; Sun, B.; Chakraborty, A. *Energy* **2015**, *91*, 772−781.
(20) Wu, H.; Simmons, J. M.; Liu, Y.; Brown, C. M.; Wang, X.-S.; Ma, S.; Peterson, V. K.; Southon, P. D.; Kepert, C. J.; Zhou, H.-C.; Yildirim, T.; Zhou, W. *Chem. - Eur. J.* **2010**, *16* (17), 5205−5214.
(21) Wilmer, C. E.; Leaf, M.; Lee, C. Y.; Farha, O. K.; Hauser, B. G.; Hupp, J. T.; Snurr, R. Q. *Nat. Chem.* **2012**, *4* (2), 83−89.

DOI: 10.1021/jacs.5b11079
J. Am. Chem. Soc. XXXX, XXX, XXX−XXX